

Effect of Long-term Low Concentrations of TiO₂ Nanoparticles on Dewaterability of Activated Sludge and the Relevant Mechanism: The Role of Nanoparticle Aging

Chengyu Jiang (✉ cy_jiang2004@163.com)

Hohai University

Qingjin Chen

Nanjing QianFu Engineering Corporation Limited

Research Article

Keywords: TiO₂ nanoparticle, Aging, Sludge dewaterability, Extracellular polymeric substance (EPS), Apoptosis, Quorum sensing

Posted Date: May 25th, 2021

DOI: <https://doi.org/10.21203/rs.3.rs-484241/v1>

License: © ⓘ This work is licensed under a Creative Commons Attribution 4.0 International License.

[Read Full License](#)

Version of Record: A version of this preprint was published at Environmental Science and Pollution Research on September 25th, 2021. See the published version at <https://doi.org/10.1007/s11356-021-16451-4>.

Abstract

Nanoparticles can undergo aging phenomena that change their physical and chemical properties in sewage treatment systems. However, the effect of aged nanoparticles under long-term low concentrations on the dewatering performance of activated sludge in sewage treatment systems has not been reported yet. Here, we compared the chronic effects of pristine and aged TiO₂ nanoparticles on sludge dewatering index including specific resistance to filtration (SRF) and bound water (BW) in the sequencing batch reactor (SBR) with the µg/L concentration levels and the relevant mechanisms were analyzed. The results show that the aging experiment in sludge supernatant could change the photosensitivity and water stability of nanoparticles, which was mainly due to the changes in the zeta potential and energy band of the particle, and ultimately attributed to the combined effect of particle surface inclusions such as organic matter and inorganic salt. At 10µg/L, nanoparticles could reduce the dewaterability of sludge, but at 100µg/L, nanoparticles could improve the dewaterability of sludge, because 10µg/L promoted the secretion of extracellular polymeric substance (EPS), regulated the structure of sludge flora and increased the abundance of secreting quorum sensing-acyl-homoserine lactones (QS-AHL) and EPS genera, while the corresponding exposure results of 100µg/L were the opposite, due to the damage and necrosis exposure effects of 100µg/L under long-term light, which reduced EPS production and increased sludge density. Interestingly, aging could alleviate the effects of two exposure concentrations on sludge dewatering, mainly being attributed to the decrease of the photoactivity of nanoparticles. The results of this study show that environmental aging could slow down, but cannot reverse the results of exposure to specific concentrations of nanoparticles. However, the ecological effects of photosensitive nanoparticles with two environmentally-relevant concentration levels of µg/L were significantly different, which should be refined and confirmed again in freshwater environment to provide a basis for subsequent scientific management and control of photosensitive nanoparticles.

1. Introduction

TiO₂ nanoparticle (TiO₂ NP) is widely used in catalysts, sunscreens, cosmetics, coatings, plastics, medicine, and environmental management due to the superior physicochemical properties (Li et al., 2020a). With the accelerated application of TiO₂ NP, wastewater treatment plants (WWTPs) will increasingly receive TiO₂ NP. Recently, it was found that the raw sewage contains approximately 100–3000 µg/L of Ti, and the concentration in sludge is even as high as 23.2 mg/kg (Gottschalk et al., 2009). Therefore, it is inevitable that TiO₂ NP would interact with microbial aggregates such as activated sludge or biofilm in WWTPs. It is reported that the WWTPs could intercept more than 95% of the TiO₂ NP, and most of that are adsorbed on the microbial aggregates surface or infiltrated into the cells (Kiser et al., 2009). This might have adverse effects on the physical and chemical properties and functional activities of microbial aggregates. Most of the previous studies were keen on short-term or high concentration acute exposure experiments. For example, TiO₂ NP with the high exposure concentrations (1 mg/L-1000 mg/L) were focused on the acute toxic effects to the microbial aggregates by inhibiting the activity of microbial aggregates (Li et al., 2019), causing a reduction in the photosynthetic efficiency (Li et al.,

2017a), screening and remodeling the structures of microbial communities (Garcia et al., 2012), and reduce the functional capacity of microbial aggregates, such as nitrogen and phosphorus removal (Li et al., 2014; Li et al., 2017b). However, there are few reports about the long-term low-concentrations exposure effect of TiO₂ NP on physical and chemical properties of microbial aggregates such as dewaterability of activated sludge in WWTPs. This is not only the key to evaluate the response and adaptation mechanism of sewage treatment system when faced with duress, but also the basis to comprehensively evaluate the sewage ecological risk of TiO₂ NP.

The ecological effect of nanomaterials is closely related to their incubation time in environmental media and surface characteristic state caused by it (Nowack et al., 2012). It is reported that nanoparticles could undergo aging process in environmental media, that is, the transformation of comprehensive characteristics (such as physicochemical properties) after experiencing complex environmental behaviors. It is worth noting that the aging conditions of nanomaterials such as TiO₂ NP and their aging experimental methods in different environmental media such as soil/sediment or organic matter have been recognized by researchers (Fan et al., 2017; Lei et al., 2016; Wang et al., 2015). For example, Li et al. (2020b) and Li et al. (2020c) have reported that TiO₂ NP could incubate and age in municipal sewage and natural surface waters, respectively, which could recreate its surface properties, and ultimately affect its water stability and photosensitivity. This might have a significant impact on its aquatic ecological effects. In term of particles water stability corresponding to the change in particle size, only when the material size is in the nano-scale range, we can call it nanomaterials, and its specific nano-effects will appear. It is reported that the surface activity and hydrophilicity of TiO₂ NP would change with the change of particle size (Wang et al., 1997b). In addition, particle size is also a key factor for long-distance transmission or short-distance penetration, which is responsible for the ecological risk of nanomaterials (Wang et al., 2019). Previous studies only focused on the toxic results of pristine nanoparticles (Dwivedi et al., 2015; Qian et al., 2017), but ignored the process effect (such as aging transformation) of nanoparticles in the environmental media such as sewage treatment system (Dwivedi and Ma, 2014). Hardly realize the change of the characteristics of nanoparticles in the exposure medium when they are incubated in the exposure system for a long time, and the changes of biological behaviors and responses caused by this particulate environmental process are unknown. Then, the leading factors and persistence of risks of nanoparticle in the exposed system are also unknown.

Furthermore, as a kind of photoactive nanomaterial, the photosensitivity of TiO₂ NP is expected to become another important ecological process in the aquatic environment (Sun et al., 2014). This not only arouses concerns of ecologists about the phototoxicity of TiO₂ NP, but also arouses their thinking about the stability of photocatalytic activity of TiO₂ NP after the change of its surface structure and functional groups regulated by long time incubation in the relevant environmental media (Pan et al., 2011; Wang et al., 1997a). It is reported that the surface properties and photosensitivity of TiO₂ NP could be changed by aging processes in sewage transportation and in freshwater environment, mainly due to the encapsulation and passivation of organic compound and inorganic ions in the corresponding water bodies (Li et al., 2020b, c). However, when TiO₂ NP end up in WWTPs and detained there for a long time,

the changes of its surface characteristics and photosensitivity are unknown, which may affect the evaluation of the persistent adverse risk of TiO₂ NP in wastewater treatment process.

In view of the above analysis, we systematically elaborated the changes in sludge dewatering performance and EPS secretion in the sequencing batch reactor activated sludge process, and related mechanisms were analyzed in terms of responses of bacterial cell death modes, quorum sensing signal and sludge density, and key microbial abundance in activated sludge after long-term low concentrations exposure of TiO₂ NP, with a particular focus on roles of changes in size and photosensitivity of aged TiO₂ NP to supplement the study of the persistent biological effects of nanoparticles with the relatively real particle states and environmentally relevant concentrations in WWTPs.

2. Materials And Methods

2.1. TiO₂ NP and reagents

Commercially bare anatase TiO₂ NP (100 nm, 99.8% purity) was obtained from Shanghai Aladdin biochemical technology Co., Ltd. All chemicals and reagents from Aladdin (Shanghai, China) used in this study were of analytical grade except for the standard products used for the drawing of specific markings such as proteins and polysaccharides.

2.2. Aging experiment of nanoparticles

Two suspensions (100µg/L) of TiO₂ NP were prepared by adding 200µg of the TiO₂ NP to 2 L (beaker) of Milli-Q water (pH = 7 ± 0.1) or filtered aerobic tank suspension (0.45µm filter membrane) collected from Tiebei WWTPs (Nanjing, China) accompanied by typical municipal water quality, and then followed by 1 h of ultra-sonication (20°C/250W/40kHz). The hydrodynamic diameters and zeta potential profiles of the TiO₂ NP in two stock suspension were then determined respectively on day 0 (dispersion state) using Malvern Zeta sizer Nano ZS90 equipment (Malvern Instruments, UK), in addition, the photo-sensitivities of TiO₂ NP in two suspensions were also detected by UV-vis spectrophotometer. Next, the two nanoparticles suspensions were stirred (200 rpm) for 300 days under the simulated sunlight with the illumination period of 12h: 12h. The evaporation of water in the beaker could be replenished at any time with Milli-Q water or filtered aerobic tank sewage. After incubation, the particle size distribution, zeta potential and photosensitivity of samples were characterized again, and then the suspensions were centrifuged to remove the supernatant and freeze-dried. The surface properties of the dried powder were characterized to explore the remodeling of the surface properties of the TiO₂ NP after incubation. High-resolution transmission electron microscopy (HRTEM) and X-ray diffraction pattern (XRD) were obtained respectively to determine the morphology, microstructure and crystalline pattern of TiO₂ NP. The aged particles have also undergone UV-visible diffuse reflectance measurement to calculate its band gap according to the previous agreement (Li et al., 2019).

2.3. Activated sludge domestication culture and exposure experiments

The activated sludge was taken from a secondary sedimentation tank at the Tiebei WWTP in Nanjing, China. The concentration of titanium (Ti) in sludge matrix is very low ($0.5 \pm 0.08 \mu\text{g Ti/g VSS}$), however, after 45 days of acclimation, Ti was almost undetectable in the sequence batch reactor (SBR), indicating the sludge was no longer preselected for titanium tolerance. After acclimatization for about 45 days, when the sludge maintained a steady operational performance with an average chemical oxygen demand (COD) removal efficiency of 96.36%. For the exposure experiment, both $10 \mu\text{g/L}$ and $100 \mu\text{g/L}$ were chosen as the environmentally relevant concentrations of TiO_2 NPs in the WWTPs, and the exposure time was 300 days (chronic exposure). Considering that WWTPs mainly operates outdoors, a simulated solar irradiation with a radiation intensity of 3.6 mW/cm^2 UVA, 0.19 mW/cm^2 UVB, and $75 \mu\text{E/m}^2\text{s}$ photosynthetically active radiation, representing environmentally realistic UV irradiation reaching the surface of water on a summer day (Schug et al., 2014), was used in the acclimation and exposure experiment of sludge, and the light cycle was 12h: 12h. For comparison, the SBR without TiO_2 NP exposure but with light was studied.

2.4. Extracellular polymeric substance (EPS) extraction and analysis

Briefly, at the end of the experiments, 25mL of activated sludge samples were suspended in 50 mL centrifuge tubes, mixed with 0.05% (w/w) NaCl solution to form a 50mL suspension, and then centrifuged at $6000 g$ for 10 min to remove the loose slime polymers attached to the surface of the activated sludge. The sludge pellets accumulated at the bottom of the centrifuge tubes was re-suspended in a 0.05% (w/w) NaCl solution, and then ultrasound was then performed for 2 min at 20 kHz. The homogeneous mixtures obtained from horizontally vibrating in a thermostat incubator at 150 rpm for 15 min was immediately centrifuged at $8000 g$ for 10 min. The supernatants were regarded as the loosely attached EPS. The residual pellets were re-suspended at their initial volume again in a 0.05% (w/w) NaCl solution followed by ultrasound for 2 min at 20 kHz, then heated at 70°C for 30 min. Finally, the suspension was centrifuged at $11,000 g$ for 30 min, and the supernatant was carefully collected as the tight binding EPS. All the EPS fractions are mixed and filtered with $0.45 \mu\text{m}$ acetate cellulose membranes and stored at -20°C before analysis. The main components of EPS, such as proteins (PRO) and polysaccharide (PS) were also quantified according to previous agreements (Qian et al., 2017).

2.5. Flow cytometry analysis

In order to verify whether the sludge cells undergo apoptosis and necrosis after long-term low concentration exposure, the physiological status of sludge cells was evaluated by multi-parameter flow cytometry using an Annexin V-FITC/PI Apoptosis Kit (AV/PI; Invitrogen) (Dwyer et al., 2012; Eray et al., 2015). Detecting the externalization of phosphatidylserine (PPS) in apoptotic bacteria using recombinant Annexin V conjugated to green-fluorescent FITC dye and dead bacteria using propidium iodide (PI) with a

red-fluorescence (Dwyer et al., 2012; Eray et al., 2015). Annexin V is a Ca^{2+} dependent phospholipid binding protein with a molecular weight of 35.8 KD. It can bind to PPS with high affinity in the process of apoptosis (Pester et al., 2012). Annexin V-FITC staining can identify apoptosis at an early stage as well as the late stages of cell death resulting from either apoptotic or necrotic processes. The preparation of the sludge single cell suspension, the staining process and the machine test are all based on the previous methods (Li et al., 2019). For staining procedure: briefly, using binding buffer (1×working) to prepare single cells suspension 100 μL with a concentration 1×10^6 - 1×10^7 cells/mL, and then incubating for 10 min after adding the 2.5 μL Annexin V-FITC at room temperature in the dark, followed by adding 5 μL PI and washed with the pre-cooled PBS immediately and analysis after incubating for 1 min at room temperature in the dark.

2.6. DNA extraction and high throughput sequencing

At the end of the exposure, sludge samples (0.5 g) were homogeneously obtained from the SBR and immediately stored at -20°C until DNA was extracted. DNA was extracted using an E.Z.N.A. Soil DNA kit (OMEGA, D5625-01, USA) based on the manufacturer's instructions. The concentrations of the extracted DNA were determined by 0.8% (w/v) agarose gel electrophoresis. The microbial communities with or without TiO_2 NP exposure were analyzed by an Illumina MiSeq platform according to standard protocols and were conducted by Guangdong Magigene Biotechnology Co., Ltd. China (Wang et al., 2018). Detailed information was available in the SI.

2.7. Other analytical methods and statistical analysis

The specific resistance to filtration (SRF) and bound water (BW) content were measured to characterize the dewatering capacity of sludge (You et al., 2017). The accumulation of intracellular nanoparticles inside the activated sludge was measured and the intracellular oxidative damage (ROS) in sludge cells was tested using the methods described in previous report (Li et al., 2019). The changes in the concentration of lactate dehydrogenase (LDH) outside the activated sludge cells were used to evaluate bacterial cytoplasmic membrane permeability. The density of activated sludge floc and quorum-sensing (QS) signaling molecule responses via acyl-homoserine lactones (AHLs) were determined. Details of the experiments and calculation methods are available in the SI.

All tests were conducted in triplicate, and the values are presented as the means \pm standard deviation. One-way analysis of variance was used to identify statistical significance ($p < 0.05$: significant and $p < 0.01$: highly significant) between the control and exposure groups or between different exposure groups.

3. Results And Discussion

3.1. Characteristics of the pristine and aged TiO_2 NP

As shown in Fig. 1a-1d, after 300 days of sludge supernatant aging experiment, HRTEM (JEM-2100F, Japan) and XRD (Model D8, Advanced X-ray diffractometer, Germany) revealed obvious changes in

surface morphology and element distribution of the TiO₂ NP. The clear crystal texture on the surface of the nanoparticles becomes fuzzy and cohesive, mainly due to the encapsulation of organic matter and inorganic salts such as NaCl in the sludge supernatant. However, the crystallinity, grain size, and arrangement of the TiO₂NP influence its original photocatalytic activity and selectivity (Vance et al., 2015), and are not affected by aging. In addition, both pristine and aged nanoparticles comprise internal monocrystalline structures with dominant crystal surface index of (101) (the figures in parentheses represent the miller indices), which doesn't seem to affect the toxic behavior of faceted TiO₂ NP in terms of its distinctive crystallographic facets (Liu et al., 2016).

Interestingly, the aging experiment in the sludge supernatant changed the light absorption capacity of the nanoparticles, which caused the red shift of the photosensitivity (Fig. 1e) and reduced the band-gap energy (E_g) of TiO₂ NP from 3.2 eV to 3.1 eV (Fig. 1f). This seems to be different from previous reports that both surface water bodies and piping sewage aging experiments could increase the E_gs of anatase nanoparticle and decrease the energy band of rutile nanoparticle (Li et al., 2020b, c). This might be attributed to the differences in aging water quality and incubation time, for example, organic substances such as humic acid in the water can photosensitize the nanoparticles (Leads and Weinstein, 2019), while the presence of salt crystals reduced the photocatalytic efficiency of TiO₂ NP by the “sheltering phenomenon of deposited salt” (Xu et al., 2019). Moreover, compared to previous studies, here, the delay of the aging time could change the composition and thickness of deposited or wrapped on the surface of the nanoparticles, to an extent, the surface microstructure and photoactivity of the nanoparticles are the result of the comprehensive regulation of the above aging behaviors (Halle et al., 2020).

In addition, Fig. S1 shows that aging can not only increase the stability of the water environment of the nanoparticles, but also increase the particle small size abundance range, which corresponds to the increase of the absolute value of the zeta potential on the surface of the aged nanoparticles. This is mainly due to the fact that the surface of the aged nanoparticles were wrapped by a large amount of negatively charged organic matter in the sludge supernatant, which increased the electrostatic repulsion and steric hindrance effects of nanoparticles (Gilbert et al., 2007).

3.2. Dewaterability and EPS secretion properties of activated sludge

Here, two indexes, the SRF and BW were to evaluate sludge dewaterability under laboratory conditions. Figure 2A shows that 10 µg/L nanoparticles could significantly ($p < 0.01$) increase the SRF, however, 100 µg/L TiO₂ NP could significantly ($p < 0.01$) reduce SRF compared with the control, and the BW contents showed a similar trends that of SRF (Fig. 2B), indicative of a severe decrease or increase in sludge dewaterability with two concentration levels of µg/L concentration levels. Interestingly, aging could reduce the influence of nanoparticles on the dewatering performance of activated sludge, for example, compared with the pristine nanoparticles, the application effects of the aged nanoparticles were significantly weakened, showing that a 10 µg/L TiO₂ NP obviously ($p < 0.05$) increase the SRF, while a

100 µg/L TiO₂ NP obviously ($p < 0.05$) decrease the SRF, and the change trend of BW is still consistent with the change trend of SRF.

It is reported that EPS, a gel-like matrix and accounts for 80% of the total sludge mass, with significant influences on sludge hydrophobicity, surface charge, microbial aggregates, flocculation, and adhesion (Liu and Fang, 2003), is the major limiting factor of sludge dewatering (Chen et al., 2015). Here, Fig. 2C shows that the amount of total EPS mainly composed of PRO and PS keep the same changing trend with that of both SRF and BW of sludge, that is to say, whether aging or not, 10 µg/L could promote the secretion of EPS, while 100 µg/L could inhibit the production of EPS, implying that EPS and sludge dewatering performance are closely related. Li et al. (2019) have reported that the composition and structure of EPS have a great influence on the dewatering performance of sludge, for example, the PRO in EPS was responsible for the change of SRF, while the change of BW was dominated by PS in EPS. Therefore, in this study, PRO and PS in EPS either increased significantly (10 µg/L, $p < 0.05$) or decreased significantly (100 µg/L, $p < 0.05$) compared to control, which explained the changing trends of SRF and BW of activated sludge in the corresponding exposure group.

3.3. Related mechanism analysis of sludge dewaterability change

3.3.1. Mode of microbial cells death in sludge and related causes

It is reported that the death mode of sludge cells is related to EPS secretion and composition, which may explain the difference of sludge dewatering performance in different exposure groups (Li et al., 2019). Figure 3A shows that there are two ways of death of sludge cells: apoptosis (cell membrane integrity) and necrosis (cell membrane leakage), which have been confirmed by previous reports (Chaloupka and Vinter, 1996; Dwyer et al., 2012). Compared with control group and exposure groups of 10 µg/L nanoparticles, 100 µg/L nanoparticles showed severe inflammatory injury, leading to significant ($p < 0.01$) leakage of LDH in sludge cells (Fig. 3B), and resulting in obvious cell necrosis (Fig. 3A). It should be noted that aging could slow down the necrosis damage of sludge cells caused by TiO₂ NP, but it seems to increase the induction of apoptosis of sludge cells (Fig. 3A). This is mainly attributed to the degradation of photo oxidation damage ability of TiO₂ NP due to aging, but the stability of aged nanoparticles in sewage environment is increased and could maintain a stable small particle size range in the sewage system (Fig. S1), and finally promoted the accumulation of particles in sludge cells (Fig. 3C) and led to intracellular peroxidation and oxidative damage (Fig. 3D). Thus, relatively, at the lethal exposure concentrations (100 µg/L), the pristine nanoparticles tended to lead to sludge cell necrosis, while the aged nanoparticles were easy to induce the apoptosis of microbial cells, which has been verified in previous studies (Li et al., 2019; Li et al., 2020b). However, as far as 10µg/L is concerned, regardless of aging or not, this exposure concentration level is not the damage concentration.

3.3.2. Changes of quorum sensing and sludge density and related causes

It is reported that the quorum-sensing (QS) information of the microbial community in the activated sludge regulates the changes in the EPS secretion and density of the sludge (Shrout and Nerenberg, 2012), which in turn will significantly affect the sludge dewatering performance (Wu and Wu, 2001; Zhang et al., 2017). Therefore, after exposure, the QS signal (AHL) response and density change of activated sludge are also monitored. Figure 4A and Fig. 4B show that in the all exposed groups, the change trends of QS-AHL secretion and sludge density was opposite, for example, 10 µg/L TiO₂ NP could improve the QS-AHL secretion and enhance sludge organic trend by improving EPS production with the decrease of sludge density, while 100 µg/L TiO₂ NP could inhibit the secretion of QS-AHL and enhance the inorganic tendency of sludge by reducing EPS production with the increase of sludge density. It is worth noting that aging could attenuate the responsiveness of QS-AHL and sludge density caused by the two concentrations of pristine nanoparticles, but it's hard to completely alleviate, and there are still significant ($p < 0.05$) levels relative to the control group (Fig. 4). This also suggested that whether aging or not, 10 µg/L concentration level of nanoparticles was promoting effects and 100 µg/L was inhibiting effects on EPS generation and physiological behavior of entire microbial communities in activated sludge, as the QS molecule was in reasonable agreement with the regulation of gene expression and the biosynthesis of EPS during mixed-species aerobic granule formation (Shrout and Nerenberg, 2012; Wang et al., 2018). In addition, QS signal secreted and differentially altered by TiO₂ NP exposed groups suggest that the social and physiological environments (community structure and diversity) of microbial population in sludge were influenced.

In view of the above analysis, this study used high-throughput sequencing technology to monitor the key genera secreting QS-AHL and genera secreting specific EPS. Firstly, as shown in Table S2, regardless of aging or not, after exposure, 10 µg/L TiO₂ NP could promote the richness and diversity of activated sludge microbial community in term of the OTUs and Shannon index, while 100 µg/L reduced the richness and diversity of microorganisms in sludge based on the Chao and Shannon index respectively, compared with the corresponding indexes of the control group. This might indicate that there are significant differences in the structure of microbial community or the evolution of specific microbial community in activated sludge after exposure to different concentrations of nanoparticles. In addition, for some bacteria, the EPS production is directly controlled by QS-AHL (Gilbert et al., 2009; Shrout and Nerenberg, 2012). In this study, the QS bacteria and some specific EPS-secreting genera in the activated sludge, directly or indirectly controlled by QS-AHL, are shown in Table 1. These QS bacterial abundances increase or decrease after exposure to TiO₂ NP with different concentrations; however, considering the increase (10 µg/L) or decrease (100 µg/L) of QS-AHL (Fig. 4A), the genera with a significant increase or decrease correspondingly in abundance (Table 1), such as *Acinetobacter*, *Aeromonas*, *Comamonas*, *Nitrobacter*, *Nitrosomonas*, *Pseudomonas*, and *Sphingomonas*, could play a key role in the secretion of AHL-signaling molecule. Moreover, the bacterial genera of *Bradyrhizobium*, *Burkholderia*, and *Sphingomonas* are responsible for the significant increase of PS, one of the main components of EPS,

while the bacterial genera of *Flavobacterium*, *Bosea*, and *Ralstonia* are responsible for the significant increase of other components such as protein in EPS in the 10 µg/L nanoparticles exposed groups. By contrast, at 100 µg/L, the abundances of the above specific EPS-secreting species were substantially decreased, which is consistent with the trend of sludge density increasing under exposure to the higher concentration (100 µg/L) (Fig. 4B). The above analysis suggests that nanoparticles could regulate bacterial community structure and secretion of signal molecule. QS bacteria and genera secreting specific EPS inside the sludge plays a key role in the QS-controlled genes relate to sludge flocs formation and density, where the bacteria emit and sense chemical signal molecules as a means to gauge population density and control EPS-gene expression (Li et al., 2020a). Thus, the dewatering performance of sludge was affected.

4. Conclusions

Our work compared the physicochemical properties and water stability of pristine and aged TiO₂ NP and the effects of aging on sludge dewatering performance after chronic exposure to TiO₂ NP at µg/L concentration level were studied, and the related mechanism was analyzed. The main conclusions are: 1) The aging experiment of nanoparticles in sludge supernatant changed the surface properties of TiO₂ NP, such as zeta potential, functional groups and energy bands, and increased the stability of the nanoparticles in water environment, but not changed the crystallinity of TiO₂ NP; 2) Regardless of aging or not, nanoparticles reduced the sludge dewaterability at the exposure concentration of 10 µg/L, and improved the sludge dewaterability at exposure concentration of 100 µg/L, but aging could weaken the effect of two exposure concentrations on sludge dewatering; 3) Exposure of nanoparticles could change the microbial community structure and the richness of both QS bacteria and genera secreting specific EPS because of the damage effect of 100 µg/L and the hormone effect of 10 µg/L with up to 300 days of exposure, leading to changes in the secretion and composition of EPS, and ultimately affecting the density and dewatering performance of the sludge. The results of this study supplement the results of long-term low concentrations of nanoparticles on the physiological and biochemical effects of microbial aggregates in sewage treatment systems, and suggesting that the impact of environmental media aging should be included in the evaluation of the ecological effects of nanoparticles because the incubation of nanoparticles in the environment is likely to affect their own ecological effects.

Declarations

Ethics approval and consent to participate

Not applicable.

Consent for publication

Not applicable.

Availability of data and materials

Not applicable.

Competing interests

The authors declare that they have no competing interests.

Funding

This study was financially supported by the Treatment Project of Black and Smelly River of Nanjing City (2017).

Authors' contributions

Chengyu Jiang designed the study, analyzed the data, and wrote the manuscript. Qingjin Chen performed the experiment and contributed to the manuscript writing.

References

1. Chaloupka, J., Vinter, V., 1996. Programmed cell death in bacteria. *Folia Microbiologica* 41, 451-464.
2. Chen, Z., Zhang, W., Wang, D., Ma, T., Bai, R., 2015. Enhancement of activated sludge dewatering performance by combined composite enzymatic lysis and chemical re-flocculation with inorganic coagulants: Kinetics of enzymatic reaction and re-flocculation morphology. *Water Research* 83, 367-376.
3. Dwivedi, A.D., Dubey, S.P., Sillanpaa, M., Kwon, Y.-N., Lee, C., Varma, R.S., 2015. Fate of engineered nanoparticles: Implications in the environment. *Coordination Chemistry Reviews* 287, 64-78.
4. Dwivedi, A.D., Ma, L.Q., 2014. Biocatalytic Synthesis Pathways, Transformation, and Toxicity of Nanoparticles in the Environment. *Critical Reviews in Environmental Science and Technology* 44, 1679-1739.
5. Dwyer, D.J., Camacho, D.M., Kohanski, M.A., Callura, J.M., Collins, J.J., 2012. Antibiotic-Induced Bacterial Cell Death Exhibits Physiological and Biochemical Hallmarks of Apoptosis. *Molecular Cell* 46, 561-572.
6. Eray, M., , Matto, M., , Kaartinen, M., , Andersson, L., , Pelkonen, J., . 2015. Flow cytometric analysis of apoptotic subpopulations with a combination of annexin V-FITC, propidium iodide, and SYTO 17. *Cytometry* 43, 134-142.
7. Fan, X.L., Wang, C., Wang, P.F., Hou, J., Qian, J., 2017. Effects of carbon nanotubes on physicochemical properties and sulfamethoxazole adsorption of sediments with or without aging

- processes. *Chemical Engineering Journal* 310, 317-327.
8. Garcia, A., Delgado, L., Tora, J.A., Casals, E., Gonzalez, E., Puentes, V., Font, X., Carrera, J., Sanchez, A., 2012. Effect of cerium dioxide, titanium dioxide, silver, and gold nanoparticles on the activity of microbial communities intended in wastewater treatment. *Journal of Hazardous Materials* 199, 64-72.
 9. Gilbert, B., Lu, G., Kim, C.S., 2007. Stable cluster formation in aqueous suspensions of iron oxyhydroxide nanoparticles. *Journal of Colloid and Interface Science* 313, 152-159.
 10. Gilbert, K.B., Kim, T.H., Gupta, R., Greenberg, E.P., Schuster, M., 2009. Global position analysis of the *Pseudomonas aeruginosa* quorum-sensing transcription factor LasR. *Molecular Microbiology* 73, 1072-1085.
 11. Gottschalk, F., Sonderer, T., Scholz, R.W., Nowack, B., 2009. Modeled Environmental Concentrations of Engineered Nanomaterials (TiO₂, ZnO, Ag, CNT, Fullerenes) for Different Regions. *Environmental Science & Technology* 43, 9216-9222.
 12. Halle, L.L., Palmqvist, A., Kampmann, K., Khan, F.R., 2020. Ecotoxicology of micronized tire rubber: Past, present and future considerations. *Science of The Total Environment* 706, 135694.
 13. Kiser, M.A., Westerhoff, P., Benn, T., Wang, Y., Perez-Rivera, J., Hristovski, K., 2009. Titanium Nanomaterial Removal and Release from Wastewater Treatment Plants. *Environmental Science & Technology* 43, 6757-6763.
 14. Leads, R.R., Weinstein, J.E., 2019. Occurrence of tire wear particles and other microplastics within the tributaries of the Charleston Harbor Estuary, South Carolina, USA. *Marine Pollution Bulletin* 145, 569-582.
 15. Lei, C., Zhang, L., Yang, K., Zhu, L., Lin, D., 2016. Toxicity of iron-based nanoparticles to green algae: Effects of particle size, crystal phase, oxidation state and environmental aging. *Environmental Pollution* 218, 505-512.
 16. Li, D.P., Cui, F.Y., Zhao, Z.W., Liu, D.M., Xu, Y.P., Li, H.T., Yang, X.N., 2014. The impact of titanium dioxide nanoparticles on biological nitrogen removal from wastewater and bacterial community shifts in activated sludge. *Biodegradation* 25, 167-177.
 17. Li, K., Qian, J., Wang, P., Wang, C., Fan, X., Lu, B., Tian, X., Jin, W., He, X., Guo, W., 2019. Toxicity of Three Crystalline TiO₂ Nanoparticles in Activated Sludge: Bacterial Cell Death Modes Differentially Weaken Sludge Dewaterability. *Environmental Science & Technology* 53, 4542-4555.
 18. Li, K., Qian, J., Wang, P., Wang, C., Le, B., Tian, X., Jin, W., He, X., Chen, H., Zhang, Y., Liu, Y., 2020a. Differential responses of encoding-amoA nitrifiers and nir denitrifiers in activated sludge to anatase and rutile TiO₂ nanoparticles: What is active functional guild in rate limiting step of nitrogen cycle? *Journal of Hazardous Materials* 384, 121388.
 19. Li, K., Qian, J., Wang, P., Wang, C., Liu, J., Tian, X., Lu, B., Shen, M., 2017a. Crystalline phase-dependent eco-toxicity of titania nanoparticles to freshwater biofilms. *Environmental Pollution* 231, 1433-1441.

20. Li, K., Qian, J., Wang, P., Wang, C., Lu, B., Jin, W., He, X., Tang, S., Zhang, C., Gao, P., 2020b. Effects of aging and transformation of anatase and rutile TiO₂ nanoparticles on biological phosphorus removal in sequencing batch reactors and related toxic mechanisms. *Journal of Hazardous Materials* 398, 123030.
21. Li, K., Qian, J., Wang, P., Wang, C., Lu, B., Jin, W., He, X., Tang, S., Zhang, C., Gao, P., 2020c. Responses of freshwater biofilm formation processes (from colonization to maturity) to anatase and rutile TiO₂ nanoparticles: Effects of nanoparticles aging and transformation. *Water Research* 182, 115953.
22. Li, Z.W., Wang, X.J., Ma, B.R., Wang, S., Zheng, D., She, Z.L., Guo, L., Zhao, Y.G., Xu, Q.Y., Jin, C.J., Li, S.S., Gao, M.C., 2017b. Long-term impacts of titanium dioxide nanoparticles (TiO₂ NPs) on performance and microbial community of activated sludge. *Bioresource Technology* 238, 361-368.
23. Liu, N., Li, K., Li, X., Chang, Y., Feng, Y., Sun, X., Cheng, Y., Wu, Z., Zhang, H., 2016. Crystallographic Facet-Induced Toxicological Responses by Faceted Titanium Dioxide Nanocrystals. *Acs Nano* 10, 6062-6073.
24. Liu, Y., Fang, H.H.P., 2003. Influences of Extracellular Polymeric Substances (EPS) on Flocculation, Settling, and Dewatering of Activated Sludge. *Critical Reviews in Environmental Science and Technology* 33, 237-273.
25. Nowack, B., Ranville, J.F., Diamond, S., Gallego-Urrea, J.A., Metcalfe, C., Rose, J., Horne, N., Koelmans, A.A., Klaine, S.J., 2012. Potential scenarios for nanomaterial release and subsequent alteration in the environment. *Environmental Toxicology And Chemistry* 31, 50-59.
26. Pan, L., Zou, J.-J., Zhang, X., Wang, L., 2011. Water-Mediated Promotion of Dye Sensitization of TiO₂ under Visible Light. *Journal of the American Chemical Society* 133, 10000-10002.
27. Pester, M., Rattei, T., Flechl, S., Gröngröft, A., Richter, A., Overmann, J., Reinholdhurek, B., Loy, A., Wagner, M., 2012. amoA-based consensus phylogeny of ammonia-oxidizing archaea and deep sequencing of amoA genes from soils of four different geographic regions. *Environmental Microbiology* 14, 525-539.
28. Qian, J., Li, K., Wang, P., Wang, C., Shen, M., Liu, J., Lu, B., Tian, X., 2017. Toxic effects of three crystalline phases of TiO₂ nanoparticles on extracellular polymeric substances in freshwater biofilms. *Bioresource Technology* 241, 276-283.
29. Schug, H., Isaacson, C.W., Sigg, L., Ammann, A.A., Schirmer, K., 2014. Effect of TiO₂ Nanoparticles and UV Radiation on Extracellular Enzyme Activity of Intact Heterotrophic Biofilms. *Environmental Science & Technology* 48, 11620-11628.
30. Shrout, J.D., Nerenberg, R., 2012. Monitoring Bacterial Twitter: Does Quorum Sensing Determine the Behavior of Water and Wastewater Treatment Biofilms? *Environmental Science & Technology* 46, 1995-2005.
31. Sun, J., Guo, L.-H., Zhang, H., Zhao, L., 2014. Irradiation Induced Transformation of TiO₂ Nanoparticles in Water: Aggregation and Photoreactivity. *Environmental Science & Technology* 48, 11962-11968.

32. Vance, M.E., Kuiken, T., Vejerano, E.P., McGinnis, S.P., Hochella, J.M.F., Rejeski, D., Hull, M.S., 2015. Nanotechnology in the real world: Redeveloping the nanomaterial consumer products inventory. *Beilstein journal of nanotechnology* 6, 1769-1780.
33. Wang, M.M., Wang, Y.C., Wang, X.N., Liu, Y., Zhang, H., Zhang, J.W., Huang, Q., Chen, S.P., Hei, T.K., Wu, L.J., Xu, A., 2015. Mutagenicity of ZnO nanoparticles in mammalian cells: Role of physicochemical transformations under the aging process. *Nanotoxicology* 9, 972-982.
34. Wang, P., Li, K., Qian, J., Wang, C., Lu, B., Tian, X., Jin, W., He, X., 2019. Differential toxicity of anatase and rutile TiO₂ nanoparticles to the antioxidant enzyme system and metabolic activities of freshwater biofilms based on microelectrodes and fluorescence in situ hybridization. *Environmental Science-Nano* 6, 2626-2640.
35. Wang, P., You, G., Hou, J., Wang, C., Xu, Y., Miao, L., Feng, T., Zhang, F., 2018. Responses of wastewater biofilms to chronic CeO₂ nanoparticles exposure: Structural, physicochemical and microbial properties and potential mechanism. *Water Research* 133, 208-217.
36. Wang, R., Hashimoto, K., Fujishima, A., Chikuni, M., Kojima, E., Kitamura, A., Shimohigoshi, M., Watanabe, T., 1997a. Light-induced amphiphilic surfaces. *Nature* 388, 431-432.
37. Wang, R., Kojima, E., Hashimoto, K., Watanabe, T., Kitamura, A., Fujishima, A., Chikuni, M., Shimohigoshi, M., 1997b. Light-induced amphiphilic surfaces. *Nature* 388, 431-432.
38. Wu, C.C., Wu, J.J., 2001. Effect of charge neutralization on the dewatering performance of alum sludge by polymer conditioning. *Water science and technology: a journal of the International Association on Water Pollution Research* 44, 315-319.
39. Xu, M., Wu, T., Tang, Y.-T., Chen, T., Khachatryan, L., Iyer, P.R., Guo, D., Chen, A., Lyu, M., Li, J., Liu, J., Li, D., Zuo, Y., Zhang, S., Wang, Y., Meng, Y., Qi, F., 2019. Environmentally persistent free radicals in PM_{2.5}: a review. *Waste Disposal & Sustainable Energy* 1, 177-197.
40. You, G., Wang, P., Hou, J., Wang, C., Xu, Y., Miao, L., Lv, B., Yang, Y., Liu, Z., Zhang, F., 2017. Insights into the short-term effects of CeO₂ nanoparticles on sludge dewatering and related mechanism. *Water Research* 118, 93-103.
41. Zhang, W., Chen, Z., Cao, B., Du, Y., Wang, C., Wang, D., Ma, T., Xia, H., 2017. Improvement of wastewater sludge dewatering performance using titanium salt coagulants (TSCs) in combination with magnetic nano-particles: Significance of titanium speciation. *Water Research* 110, 102-111.

Table

Due to technical limitations, table 1 is only available as a download in the Supplemental Files section.

Figures

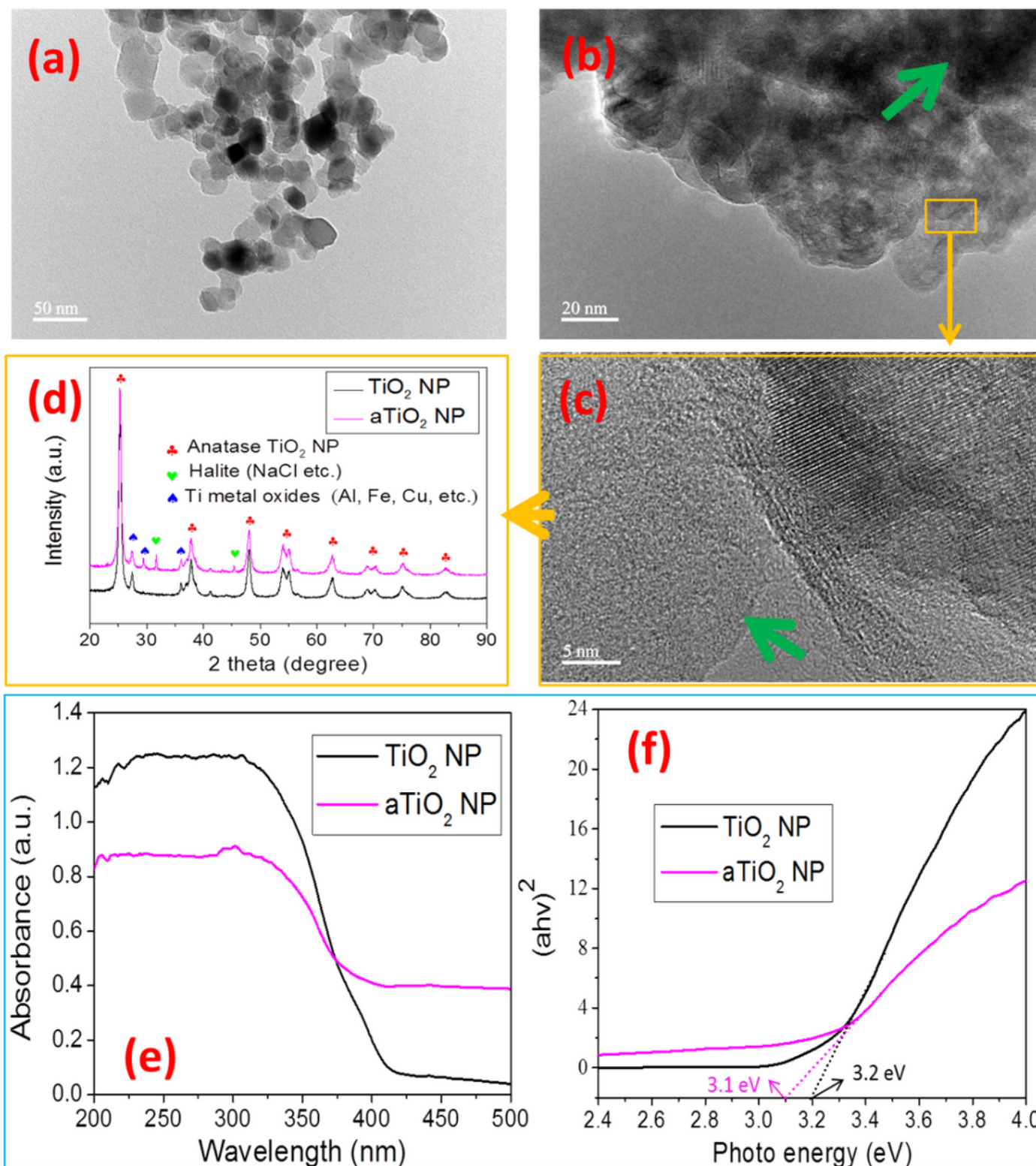


Figure 1

Physicochemical transformation of the crystalline phase of TiO₂ NP after 300 days of aging. The TEM image of pristine TiO₂ NP (Fig. 1a) and the TEM image of aged TiO₂ NP (Fig. 1b) as well as locally enlarged TEM image (Fig. 1c) with corresponding XRD patterns (squares indicated) (Fig. 1d). Green arrows represent inclusions of aged NPs. The UV-Vis diffuse reflections (Fig. 1e) of TiO₂ NP and corresponding band gaps (Fig. 1f).

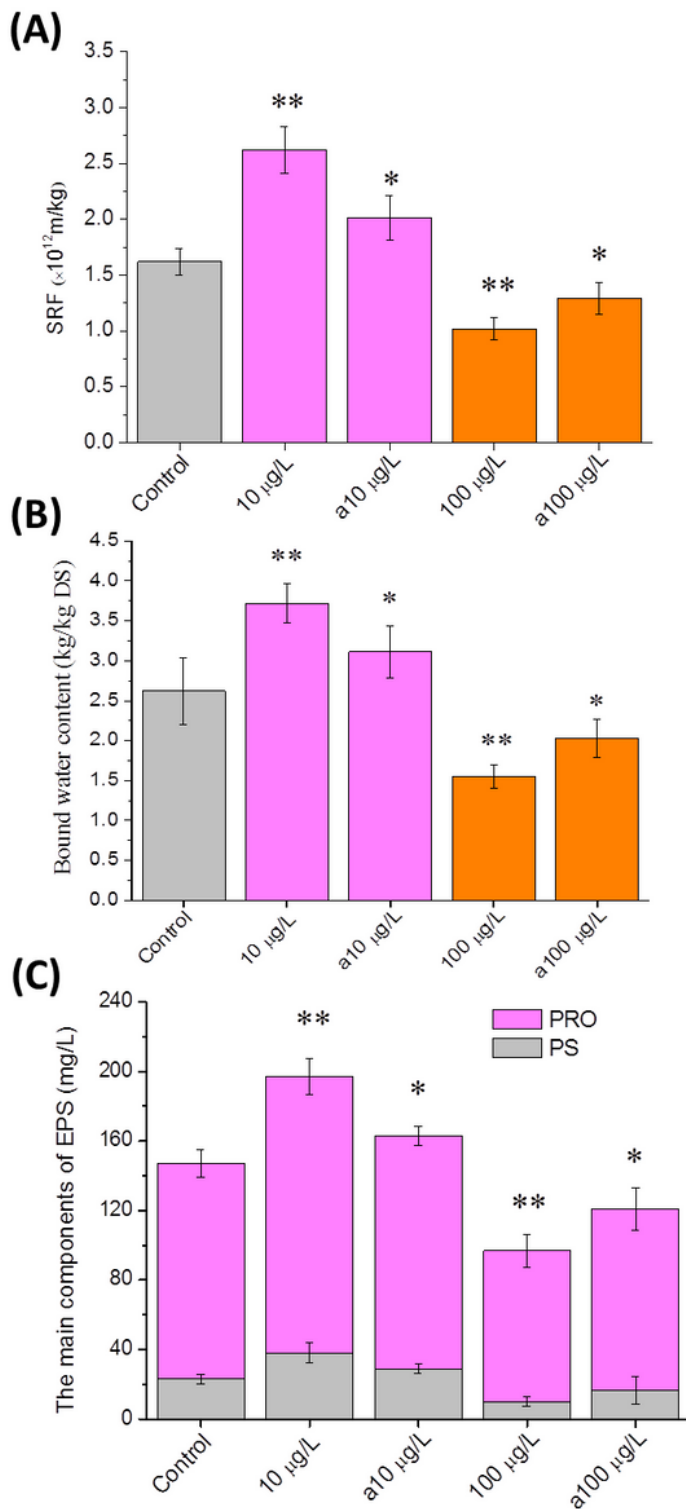


Figure 2

Effects of TiO₂ NP with or without aging on the SRF (A) and BW contents (B) as well as EPS compositions (C). Single asterisk and double asterisks indicate the statistical difference (p < 0.05) and high significance (p < 0.01) from the control, respectively. Note: a 10 µg/L and a 100 µg/L represent the exposure concentrations of aged nanoparticles, respectively. Error bars represent standard deviations (n = 3).

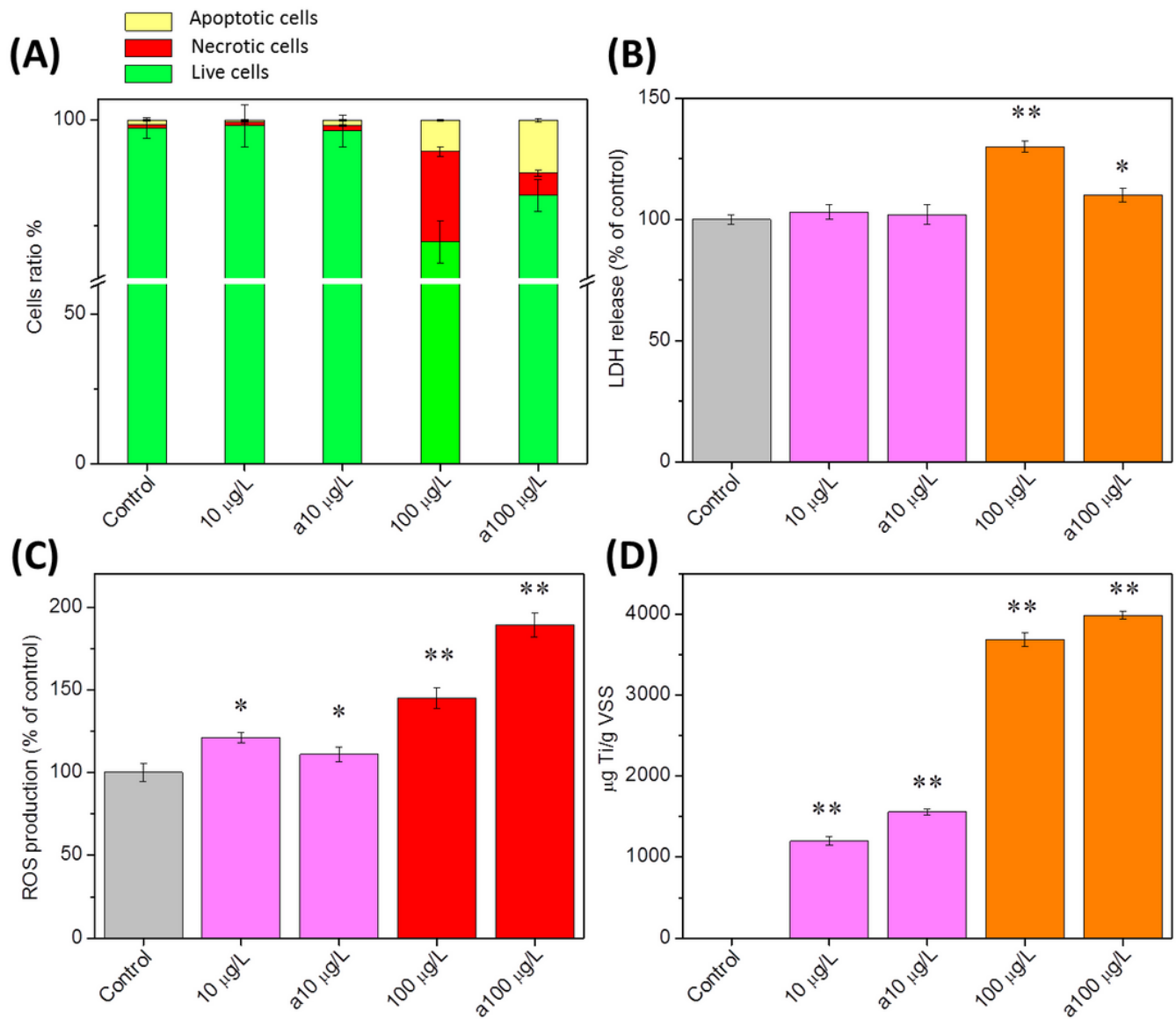


Figure 3

Analysis of the death mode of sludge cells after nanoparticle exposure (A); The LDH release in different exposure groups (B); The oxidative stress (ROS) induced in TiO₂ NP treated bacterial cells (C); The intracellular titanium concentration in activate sludge (D). Single asterisk and double asterisks indicate the statistical difference ($p < 0.05$) and high significance ($p < 0.01$) from the control, respectively. Error bars represent standard deviations ($n = 3$).

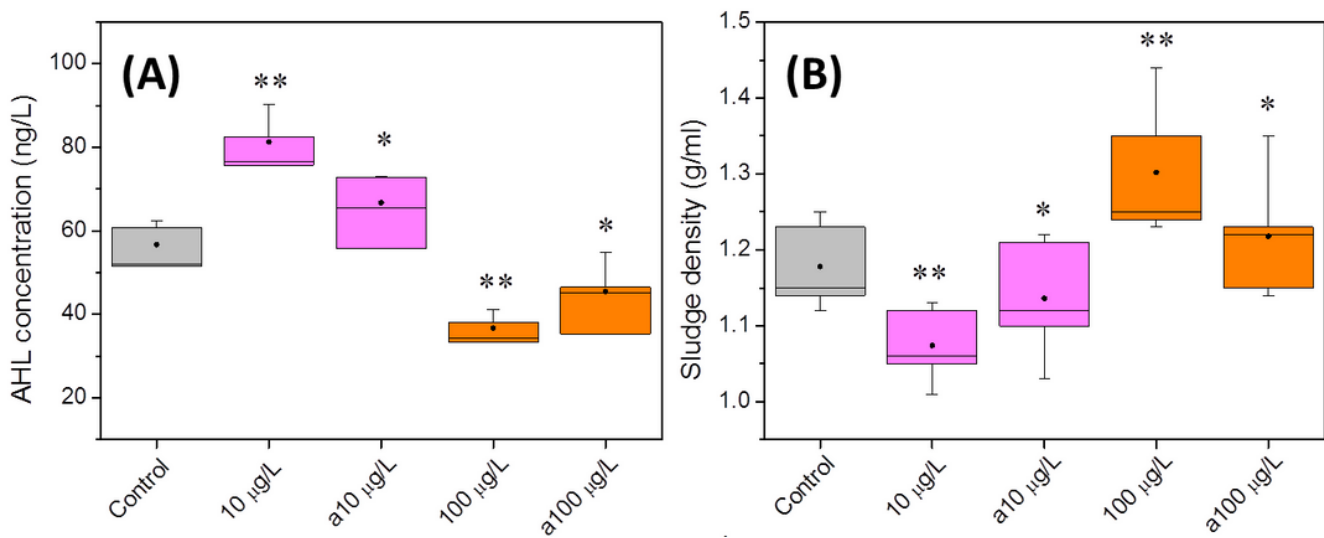


Figure 4

Effects of TiO₂NP on quorum sensing (A) and sludge density (B) of activated sludge. Single asterisk and double asterisks indicate the statistical difference ($p < 0.05$) and high significance ($p < 0.01$) from the control, respectively. Error bars represent standard deviations ($n = 3$).

Supplementary Files

This is a list of supplementary files associated with this preprint. Click to download.

- [Table1.docx](#)
- [0430Appendix.docx](#)